STEM and EDXS characterisation of physico-chemical reactions at the periphery of sol-gel derived Zn-substituted hydroxyapatites during interactions with biological fluids.

Edouard Jallot, Jean-Marie Nedelec, Anne S. Grimault, Emmanuelle Chassot, Alexia Grandjean-Laquerriere, Patrice Laquerriere, Dominique Laurent-Maquin

STEM and EDXS characterisation of physico-chemical reactions at the periphery of sol-gel derived Zn-substituted hydroxyapatites during interactions with biological fluids

E. JALLOT[1*], J.M. NEDELEC[2], A.S. GRIMAULT[1], E. CHASSOT[1], A. GRANDJEAN-LAQUERRIERE[3], P. LAQUERRIERE[3], D. LAURENT-MAQUIN[3].

[1]Laboratoire de Physique Corpusculaire de Clermont-Ferrand CNRS/IN2P3 UMR 6533
Université Blaise Pascal - 24 avenue des Landais, 63177 Aubiere Cedex, France

[2]Laboratoire des Matériaux Inorganiques CNRS UMR 6002
Université Blaise Pascal - 24 avenue des Landais, 63177 Aubiere Cedex, France

[3]INSERM – ERM 0203, Laboratoire de Microscopie Electronique, 21, rue Clément Ader, BP 138, 51685 Reims, Cedex 2, France.

*** Corresponding author** :

Edouard JALLOT

Laboratoire de Physique Corpusculaire de Clermont-Ferrand CNRS/IN2P3 UMR 6533
Université Blaise Pascal - 24 avenue des Landais, 63177 Aubiere Cedex, France.

Tel : 33 (0)4 73 40 72 65

Fax : 33 (0)4 73 26 45 98

E-mail : jallot@clermont.in2p3.fr

Hal-Inserm Author manuscript

Abstract

With its good properties of biocompatibility and bioactivity hydroxyapatite (HA) is highly used as bone substitutes and as coatings on metallic prostheses. In order to improve bioactive properties of HA we have elaborated Zn^{2+} doped hydroxyapatite. Zn^{2+} ions substitute for Ca^{2+} cations in the HA structure and four Zn concentrations (Zn/Zn+Ca) were prepared 0.5, 1, 2, 5 % at. To study physico-chemical reactions at the materials periphery, we immersed the bioceramics into biological fluids for delays from 1 day to 20 days. The surface changes were studied at the nanometer scale by scanning transmission electron microscopy associated to energy dispersive X-ray spectroscopy. After 20 days of immersion we observed the formation of a calcium-phosphate layer at the periphery of the HA doped with 5% of zinc. This layer contains magnesium and its thickness was around 200 nm. Formation of this Ca-P-Mg layer represents bioactivity properties of the 5% Zn-substituted hydroxyapatite. This biologically active layer improves properties of HA and will permit a chemical bond between the ceramic and bone.

Keywords: hydroxyapatite – zinc – bioactivity - electron probe microanalysis – sol-gel

Hal-Inserm Author manuscript

Hal-Inserm Author manuscript

Introduction

Hydroxyapatite (HA; $Ca_{10}(PO_4)_6(OH)_2$), a synthetic material analogous to calcium phosphate found in bone is considered for orthopaedic and dental applications [1, 2]. This biomaterial is highly biocompatible and presents bioactive properties. HA physicochemically bonds to bone and promotes bone formation necessary for implant osseointegration [3-6]. This property of osseointegration is needed to minimize damages to surrounding tissues and to increase the implant efficiency.

However, biological and physicochemical properties of HA can be improved by the substitution with ions usually present in natural apatites of bone. Most natural apatites are non-stoichiometric because of the presence of minor constituents such as cations (Mg^{2+}, Mn^{2+}, Zn^{2+}, Na^{+}, Sr^{2+}) or anions (HPO_4^{2-} or CO_3^{2-}) [7, 8]. Trace ions substituted in apatites can have effect on the lattice parameters, the crystallinity, the dissolution kinetics and other physical properties of apatites [9-13]. Synthesis of Zn substituted hydroxyapatite is of major interest because biological tissues like bone and teeth are composed with hydroxyapatite containing zinc. Zinc is present in small amount in the enamel of human teeth and in bone [14]. This element is probably the most important element in medicine because of its role in as much as 200 enzymes [15]. Thus, elevated concentrations in areas of damage tissues or inflammatory lesions could enhance ATP-mediated response [16].

Numerous strategies have been proposed to prepare HA. The most known and used is the precipitation method. Another method is the sol-gel technique which permits the preparation of highly pure powder due to the possibility of a strict control of the process parameters. This method offers a molecular mixing of the calcium and phosphorus precursors which is capable of improving the chemical homogeneity [17]. Moreover, the sol-gel technique allows to easily dope HA with trace elements like zinc.

Hal-Inserm Author manuscript

The purpose of the present paper is to report the synthesis of Zn-substituted hydroxyapatite and to characterize physico-chemical reactions at the ceramic periphery during interactions with biological fluids. We prepared several HA with different concentrations of zinc by the sol-gel process. Physico-chemical reactions and bioactive properties of Zn-containing are studied during interactions between HA powders and biological fluids. Knowledge of the elemental distribution at the hydroxyapatite periphery is important to understand the physico-chemical mechanisms during interactions with biological fluids. Chemical evaluation of the hydroxyapatite/biological fluids interface was performed by Scanning Transmission Electron Microscopy (STEM) associated to Energy Dispersive X-ray Spectroscopy (EDXS). These two methods are especially suitable for the study of this kind of interactions at the nanometer scale [18, 19].

Materials and Methods

Preparation and characterisation of Zn-substituted hydroxyapatite

To produce 2 mg of pure HA powder, 4.7 g of $Ca(NO_3)_2.4H_2O$ (Aldrich, USA), 0.84 g of P_2O_5 (Avocado Research chemicals, UK) were dissolved in ethanol under stirring and under reflux at 85°C during 24 h. Then, this solution was kept at 55°C during 24 h, to obtain a white consistent gel and further heated at 80°C during 10 h to obtain a white powder. Finally, the powder was heated at 1100°C during 15 h. To prepare Zn-substituted hydroxyapatite, $Zn(NO_3)_2.6H_2O$ (Acros Oraganics, UK) was added to the solution. Four Zn-substituted hydroxyapatites were prepared with Zn-substitution of 0.5, 1, 2, and 5% at. (respectively noted: HAZn0.5, HAZn1, HAZn2, HAZn5).

The chemical composition of the hydroxyapatite powders were determined by ICP-AES (Inductively Coupled Plasma-Atomic Emission Spectrometry). The nominal and experimental compositions of the five hydroxyapatites are listed in table 1.

The nature of the crystal phase was determined by powder X-ray diffraction (XRD) using a monochromatic Cu K_α radiation. The samples were scanned in the 2θ range of 10-70° on a Siemens D5000 diffractometer working in the Bragg-Brenatno configuration. X-ray diffraction patterns exhibited the peaks corresponding to hydroxyapatite. A small amount of tricalcium phosphate ($Ca_3(PO_4)_2$) was observed.

Scanning Electron Microscopy Analysis

The hydroxyapatite powders were deposited on carbon disks and sputter-coated with 20 nm of gold. Then, the samples were examined using a JEOL JSM-5910 LV scanning electron microscope at an accelerating voltage of 15 kV. All the images were recorded using the secondary electron detector.

Sample treatment

The hydroxyapatite powders (2 mg) were immersed at 37°C for 1, 2, 5, 10, and 20 days in 3 ml of a standard Dulbecco's Modified Eagle Medium (DMEM, VWR International S.A.S., France) (pH : 7.3). DMEM contained the following ingredients (mg/l): 6400 NaCl, 400 KCl, 200 $CaCl_2$, 200 $MgSO_4$-$7H_2O$, 124 NaH_2PO_4, 3700 $NaHCO_3$.

Specimen preparation and X-ray microanalysis

After treatment the hydroxyapatite powder was lying on the bottom of the box. The medium was carefully removed and the hydroxyapatite powder was embedded in resin (AGAR, Essex, England). Thin sections of 100 nanometers nominal thickness were prepared by means of a FC 4E Reichert Young ultramicrotome. The sections were placed on a copper grid (200 Mesh). Sections were coated with a conductive layer of carbon in a sputter coater to avoid charging effects.

Hal-Inserm Author manuscript

The sections were studied with a Scanning Transmission Electron Microscope (Philips CM30) operating at a voltage of 100 kV. The microscope is fitted with an energy dispersive X-ray spectrometer (EDAX 30 mm² Si(Li) R-SUTW detector). Elemental profiles from the centre to the periphery of the particles were performed using Energy Dispersive X-ray spectrometry (EDXS). The concentration profiles were made across three different particles. The elemental composition was determined by using the Cliff and Lorimer method [20, 21]. The calibration procedure was performed with standards. Concentrations are expressed in $mmol.kg^{-1}$ of resin embedded material.

Results

A pure hydroxyapatite and four Zn-substituted hydroxyapatites were prepared by sol-gel method. After heat treatment, crystalline hydroxyapatite powders are obtained with a good agreement between experimental concentrations of Ca, P and Zn determined by ICP-AES and the nominal ones (table 1). In particular, the doping with Zn^{2+} ions appears to be very efficient which is another advantage of using soft chemistry routes like sol-gel process. On SEM micrograph, we observe a hydroxyapatite particle with micropores (figure 1). All the prepared hydroxyapatites exhibit the same porous morphology.

At each immersion time, images of hydroxyapatite particles periphery were recorded by STEM. Weight concentrations gradients in Ca, P, Zn and Mg at the hydroxyapatite particles / biological fluid interface were studied by EDXS at each time of exposure to DMEM. For each immersion delay, three weight concentration profiles were acquired on three different particles. Results are characterized by an excellent reproducibility, with a standard deviation under 5 %.

Figure 2 shows the STEM micrograph of a pure hydroxyapatite particle after 20 days of immersion in DMEM. The particle looks homogeneous and is the same as the particles that

Hal-Inserm Author manuscript

we can observe before immersion in DMEM and at 1, 2, 5, 10 days after immersion in DMEM. Figures 3 and 4 show the distribution of Ca and P concentrations across the periphery of HA particles before immersion in DMEM (figure 3) and after 20 days of immersion in DMEM (figure 4). Ca and P concentrations stay constant across the periphery of HA particles for these two delays and we observed the same results for other intermediate times of exposure to the biological solution. Tables 2 and 3 present Ca, P concentrations in the centre of hydroxyapatite particles of various compositions before immersion in DMEM (table 2) and after 20 days of immersion in DMEM (table 3). No differences were observed between these two delays. The Ca/P atomic ratio is near 1.7 and corresponds to the nominal value of pure hydroxyapatite (table 1).

Concerning HAZn0.5, HAZn1 and HAZn2, we obtain similar results. The particles appear homogeneous at each delay and concentrations of Ca, P, Zn stay constant across the periphery of the different particles and in their centre (tables 2 and 3). Finally, we do not observe any formation of specific layers at their periphery for any immersion time.

Figure 5 shows the STEM micrograph of a HAZn5 particle before immersion in DMEM. The particle appears homogeneous and is the same as the particles that we can observe at 1, 2, 5, 10 days after immersion in DMEM. The distribution of Ca, P and Zn concentrations across the periphery of HAZn5 particles before immersion in DMEM is constant (figure 6). We found the same results at 1, 2, 5, 10 days after immersion in DMEM (data not shown). The STEM micrograph of a HAZn5 particle after 20 days of immersion in DMEM shows no structural changes in the centre of the particle (figure 7). However, we can observe a layer at the periphery of the HAZn5 particle. Elemental weight concentrations profiles of Ca, P, Zn and Mg reveal two zones from the centre to the periphery of HAZn5 particles (figure 8). The centre contains Ca, P, Zn elements and the concentrations stay constant. At the surface, there is a decrease in Ca and P concentrations and the Ca/P atomic

Hal-Inserm Author manuscript

ratio is of the order of 1.1. This ratio is under Ca/P atomic ratios in HA (1.67) or in TCP (1.5) and near the ratio in $CaHPO_4$. In this zone, there is no zinc and we observe the apparition of magnesium. After 20 days of immersion in DMEM, there is the formation of a Ca-P-Mg layer at the periphery of HAZn5. The thickness of this layer is of the order of 200 nm. Ca, P, Zn concentrations in the centre of HAZn5 particles evolve with time of exposure to DMEM (tables 2 and 3). Comparison of Ca, P, Zn concentrations before immersion in DMEM and after 20 days of immersion in DMEM demonstrates a significant decrease of all the concentrations.

Discussion

The present work analyzes the surface changes of pure hydroxyapatite and Zn-substituted hydroxyapatite particles immersed into biological fluid. Thanks to the sol-gel method we are able to elaborate pure hydroxyapatite and Zn-substituted hydroxyapatite powders with a good chemical homogeneity. Four hydroxyapatites doped with Zn were obtained with a good agreement between nominal and experimental concentrations. To elucidate mechanisms of interaction between hydroxyapatite and biological fluids a physico-chemical approach is adopted, namely the analysis of the transformation kinetics of the particles periphery by means of STEM-EDXS. STEM associated to EDXS allow us to determine concentration profiles at the nanometer scale. Elemental concentrations across the periphery of hydroxyapatite particles show the physico-chemical reactions occurring at the surface of the HA in contact with biological fluids.

At the different exposure times, no physico-chemical changes are observed at the interface between DMEM and HA, HAZn0.5, HAZn1, HAZn2. On the other hand, interactions between the HAZn5 and biological fluids lead to hydroxyapatite dissolution. The ionic substitution influences the dissolution process. 5% of Zn^{2+} substituted into the apatite

lattice causes changes in its physico-chemical properties. The increase in Zn concentration leads to a higher dissolution rate of hydroxyapatite. Ca deficient hydroxyapatites are more soluble than stoichiometric hydroxyapatites. Dissolution results in the leaching of Ca, P, Zn elements and to changes in the materials at the micrometer and nanometer level. Ca, P, Zn concentrations decrease in HAZn5 particles and there is the formation of a Ca-P-Mg layer at their periphery. This layer is depleted in zinc and has a thickness around 200 nm after 20 days of exposure to DMEM. This phenomenon can be described as the bioactivity process [22].

The bioactivity process occurs at the material surface. Ca^{2+}, PO_4^{3-}, Zn^{2+} ions are released and free to combine with other ions from biological fluids to form other calcium phosphate phases. After 20 days of exposure to DMEM the Ca/P atomic ratio is near 1.1 which demonstrates an accumulation of Ca^{2+} and PO_4^{3-} ions at the materials periphery. Concentrations of calcium and phosphorus increase in the surrounding fluids and this supersaturation can induce reprecipitation of other calcium phosphate crystals (brushite, octacalcium phosphate, carbonated-hydroxyapatite …) at the ceramic surface. These crystals may incorporate Ca^{2+}, Mg^{2+}, CO_3^{2-}, PO_4^{3-} and organic molecules (proteins) present in the surrounding fluids [23]. During spontaneous precipitation of Ca-P, presence of Mg^{2+}, CO_3^{2-} or organic molecules and/or supersaturation effect may promote or suppress formation of calcium phosphate *in vivo* [24]. In our case, we observe the presence of Mg in the calcium phosphate layer. Magnesium is one of the most important ions associated with biological calcium phosphates and it can play an important role during spontaneous formation of *in vivo* calcium phosphate and bone bonding [25]. The presence of Mg^{2+} stabilizes brushite, octacalcium phosphate and reduces their transformation into apatite [26, 27].

This paper demonstrates for the first time, to our knowledge, the formation of a Ca-P-Mg layer at the periphery of 5% Zn substituted hydroxyapatite. The formation of biologically relevant calcium phosphates is important for bone bonding [28]. They support the production

of an extra-cellular matrix (collagenous and non-collagenous proteins). Then the collagen fibrils are mineralized together with the incorporation of the newly formed apatite crystals in the newly formed bone [4, 29]. These reactions permit a strong chemical bond with newly formed bone at the implant/bone interface [6].

Conclusion

Synthesis of ion substituted hydroxyapatite is of major interest because biological tissues like bone and teeth are composed with hydroxyapatite containing various kinds of inorganic substances.

HA doped with 5% of Zn dissolves more rapidly than pure HA or HA doped with low concentrations of Zn. Moreover, this concentration of Zn leads to the formation of a Ca-P layer which contains Mg. This layer is created in a biological environment and represents bioactive properties of the bioceramic. The prerequisite for hydroxyapatite to bond chemically to living bone is the formation of biologically active calcium phosphates on their surface in the body. The Ca-P layer bridges chemically the bone and the implant. The reactions between hydroxyapatite and bone, and dependence of these reactions on the hydroxyapatite composition are important in bioactivity mechanisms. This paper demonstrates an increase of bioactive properties of HA doped with 5% of Zn.

Hal-Inserm Author manuscript

References

[1] M. Jarcho, J.F. Kay, K.I. Grumaer, R.H. Doremus and H.P. Drobeck, J. Bioeng. 2 (1977) 79.

[2] J.M. Sautier, J.R. Nefussi and N. Forest, Cells and Materials 1 (1991) 209.

[3] H.N. Denissen, K. De Groot, P.C. Makkes, A. Van Den Hoof and P.J. Klopper, J. Biomed. Mater. Res. 14 (1980) 730.

[4] J.M. Sautier, J.R. Nefussi and N. Forest, Biomaterials 12 (1992) 400.

[5] G. Daculsi, Biomaterials 19 (1998) 1473.

[6] R.Z. Legeros and G. Daculsi, in T. Yamamuro, L.L. Hench and J. Wilson (eds), Handbook of bioactive ceramics, vol. 2, CRC Press, Boca raton 1990.

[7] I. Mayer and J.D.B. Featherstone, J. Cryst. Growth 219 (2000) 98.

[8] S. Ben Abdelkader, I. Khattech, C. Rey and M. Jemal, Thermochimica Acta 376 (2001) 25.

[9] G. Daculsi, R.Z. Legeros, M. Heughebaert and I. Barbieux, Calcified Tissue Int. 46 (1990) 20.

[10] I.R. Gibson, K.A. Hing, J.D. Revell, J.D. Santos, S.M. Best and W. Bonfield, Key Eng. Mater. 203 (2002) 218.

[11] M. Okazaki, Biomaterials 16 (1995) 703.

[12] I.R. Gibson and W. Bonfield, J. Biomed. Mater. Res. 59 (2002) 697.

[13] E. Bertoni, A. Bigi, G. Cojazzi, M. Gandolfi, S. Panzavolta and N. Rover, J. Inorg. Biochem. 29 (1998) 72.

[14] E. Jallot, J.L. Irigaray, H. Oudadesse, V. Brun, G. Weber and P. Frayssinet, Eur. Phys. J. AP 6 (1999) 205.

[15] J.F. Zazo, Med. Hyg. 51 (1993) 2304.

[16] Li Chaoying, W. Robert, Li Zhiwang and F. Weight Forest, Proc. Natl. Acad. Sci. 90 (1993) 8264.

[17] G. Bezzi, G. Celotti, E. Landi, T.M.G. La Toretta, I. Sopyan and A. Tamperi, Mater. Chem. Phys. 78 (2003) 816.

[18] E. Jallot, H. Benhayoune, L. Kilian, Y. Josset and G. Balossier, Langmuir 17 (2001) 4467.

[19] E. Jallot, H. Benhayoune, L. Kilian and Y. Josset, Langmuir 19 (2003) 3840.

[20] G. Cliff and G.W. Lorimer, J. Microsc. 103 (1975) 203.

[21] P. Laquerriere, V. Banchet, J. Michel, K. Zierold, G. Balossier and P. Bonhomme, Microscopy Research and Technique 52 (2001) 231.

[22] B.M. Tracy and R.H. Doremus, J. Biomed. Mater. Res. 18 (1984) 719.

[23] R.Z. Legeros, R. Kijkowska, T. Abergas and J.P. Legeros, J. Dent. Res. 65 (1986) 293.

[24] R.Z. Legeros, Prog. Crystal Growth Charact. 4 (1981) 1.

[25] R.Z. Legeros, R. Kijkowska, I. Kattech, M. Jemal and J.P. Legeros, J. Dent. Res. 65 (1986) 783.

[26] E. Jallot, Applied Surface Science 211 (2003) 89.

[27] R.E. Wuthier, G.S. Rice, J.E.B. Wallace, R.L. Weaver, R.Z. Legeros and E.D. Eanes, Calcified Tissue Int. 37 (1981) 401.

[28] W. Kybalczyc, J. Christoffersen, M.R. Christoffersen, A. Zielenkiewicz and W. Zielenkiewicz, J. Cryst. Growth 106 (1990) 355.

[29] G.C.L. De Lange, C. De Putter and F.L.J.A. De Wijs, J. Biomed. Mater. Res. 24, 829 (1990).

Hal-Inserm Author manuscript

Tables

	HA	HAZn0.5	HAZn1	HAZn2	HAZn5
Ca nominal	39.88	39.63	39.38	38.88	37.41
Ca experimental	38.46 ± 1.92	38.33 ± 1.92	37.23 ± 1.86	38.13 ± 1.91	36.81 ± 1.84
P nominal	18.50	18.48	18.45	18.41	18.27
P experimental	17.21 ± 0.86	17.51 ± 0.88	17.75 ± 0.89	17.61 ± 0.88	17.08 ± 0.85
Zn theoretical	-	0.5	1	2	5
Zn experimental	-	0.45 ± 0.03	0.90 ± 0.05	1.79 ± 0.08	4.59 ± 0.23
Ca/P nominal (atomic)	1.67	1.66	1.65	1.64	1.59

Table 1 : Nominal and experimental concentrations (weight %) of Ca, P, Zn in HA, HAZn0.5, HAZn1, HAZn2 and HAZn5 determined by ICP-AES.

	HA	HAZn0.5	HAZn1	HAZn2	HAZn5
Ca	9977 ± 104	9880 ± 214	9968 ± 137	9775 ± 296	9460 ± 102
P	5888 ± 90	5991 ± 106	5935 ± 129	5923 ± 105	5941 ± 107
Zn	-	92 ± 53	245 ± 85	365 ± 115	782 ± 58
Ca/P	1.69 ± 0.05	1.65 ± 0.06	1.68 ± 0.06	1.65 ± 0.08	1.60 ± 0.05

Table 2 : Concentrations (mmol.kg^{-1} of resin embedded material) of Ca, P, Zn in the centre of HA, HAZn0.5, HAZn1, HAZn2 and HAZn5 before immersion in DMEM (mean of 10 values).

	HA	HAZn0.5	HAZn1	HAZn2	HAZn5
Ca	9904± 131	9998 ± 184	9990 ± 188	9837 ± 111	8984 ± 197
P	5931 ± 164	5969 ± 125	5934 ± 124	5904 ± 174	5623 ± 150
Zn	-	93 ± 32	218 ± 65	367 ± 45	569 ± 124
Ca/P	1.67 ± 0.07	1.67 ± 0.07	1.68 ± 0.07	1.66 ± 0.07	1.60 ± 0.08

Table 3 : Concentrations (mmol.kg^{-1} of resin embedded material) of Ca, P, Zn in the centre of HA, HAZn0.5, HAZn1, HAZn2 and HAZn5 after 20 days of immersion in DMEM (mean of 10 values).

Hal-Inserm Author manuscript

Figure captions

Figure 1 : SEM micrograph of a hydroxyapatite doped with 5% of Zn (HAZn5).

Figure 2 : STEM micrograph of a pure hydroxyapatite after 20 days of immersion in DMEM (HA : hydroxyapatite). The white dashed line represents the spectra acquisition line, where X corresponds to the position of the first recorded spectrum.

Figure 3 : Elemental concentrations ($mmol.kg^{-1}$) profiles of Ca and P across the periphery of hydroxyapatite particles before immersion in DMEM (mean of three weight concentration profiles across three different particles, standard deviation is under 5 %).

Figure 4 : Elemental concentrations ($mmol.kg^{-1}$) profiles of Ca and P across the periphery of hydroxyapatite particles after 20 days of immersion in DMEM (mean of three weight concentration profiles across three different particles, standard deviation is under 5 %).

Figure 5 : STEM micrograph of a hydroxyapatite doped with 5% of zinc before immersion in DMEM (HAZn5). The white dashed line represents the spectra acquisition line, where X corresponds to the position of the first recorded spectrum.

Figure 6 : Elemental concentrations ($mmol.kg^{-1}$) profiles of Ca, P and Zn across the periphery of HAZn5 particles before immersion in DMEM (mean of three weight concentration profiles across three different particles, standard deviation is under 5 %).

Figure 7 : STEM micrograph of a hydroxyapatite doped with 5% of zinc after 20 days of immersion in DMEM (HAZn5). The white dashed line represents the spectra acquisition line, where X corresponds to the position of the first recorded spectrum.

Figure 8 : Elemental concentrations (mmol.kg^{-1}) profiles of Ca, P, Zn and Mg across the periphery of HAZn5 particles after 20 days of immersion in DMEM (mean of three weight concentration profiles across three different particles, standard deviation is under 5 %).

Hal-Inserm Author manuscript

Hal-Inserm Author manuscript

Figures

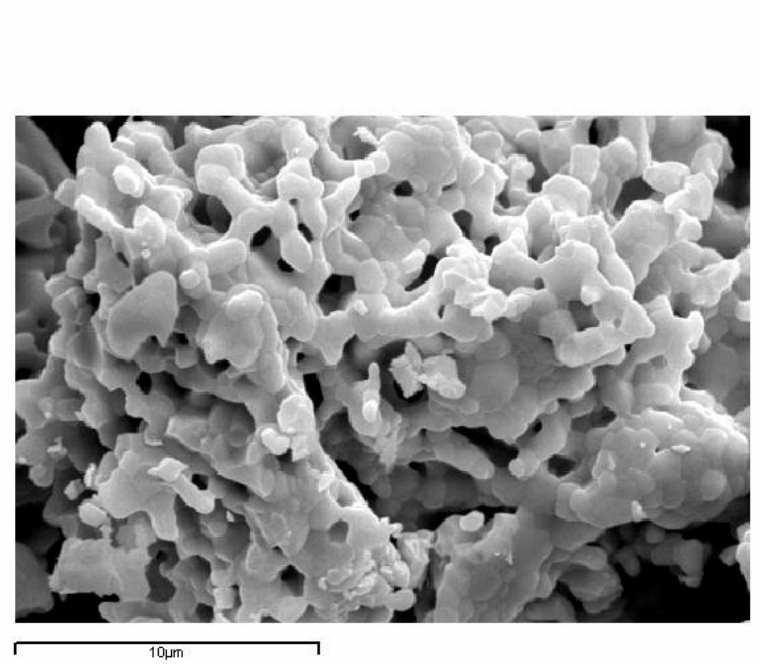

Figure 1

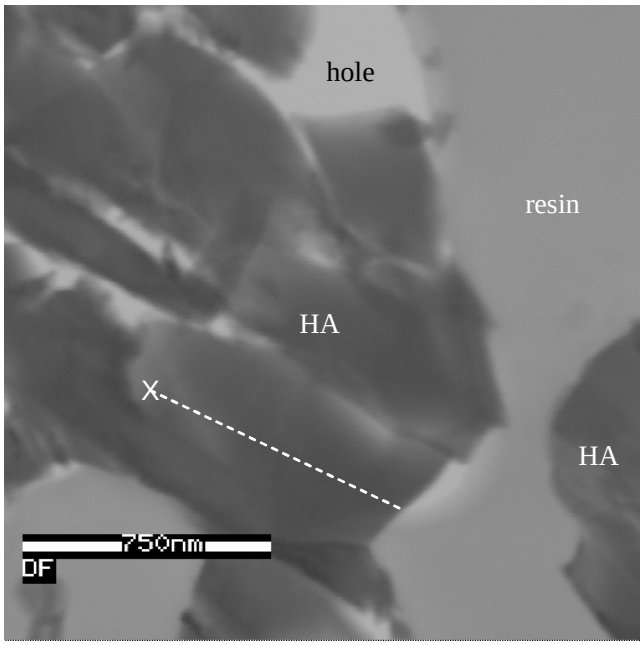

Figure 2

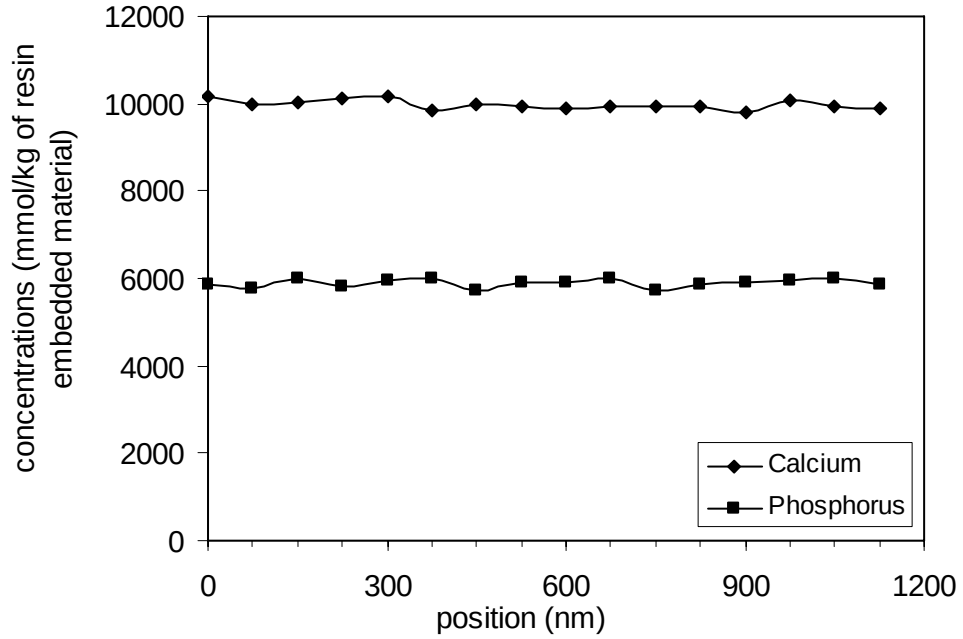

Figure 3

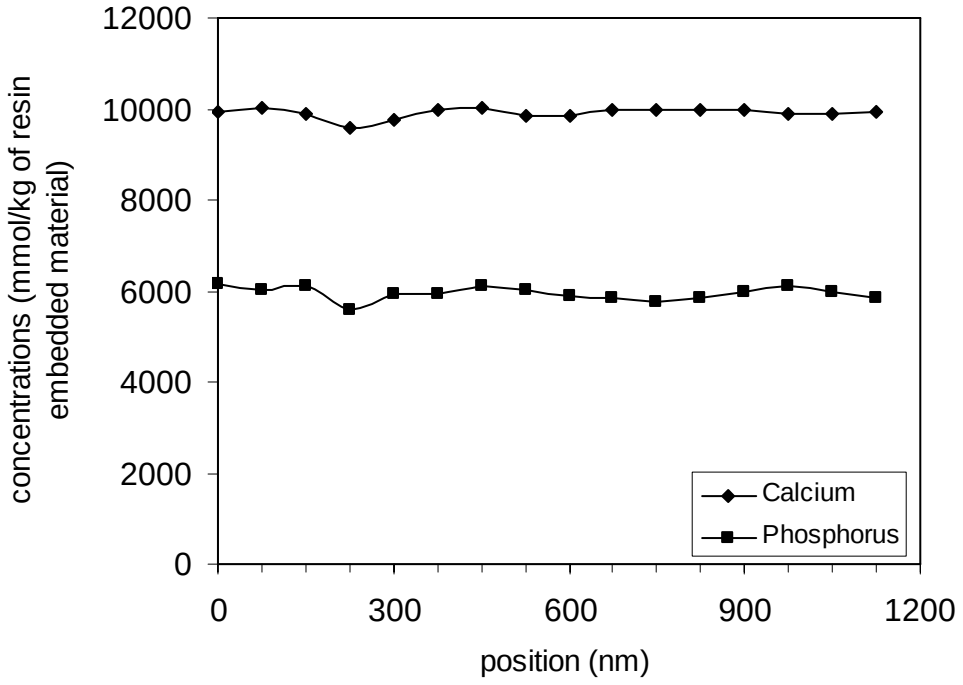

Figure 4

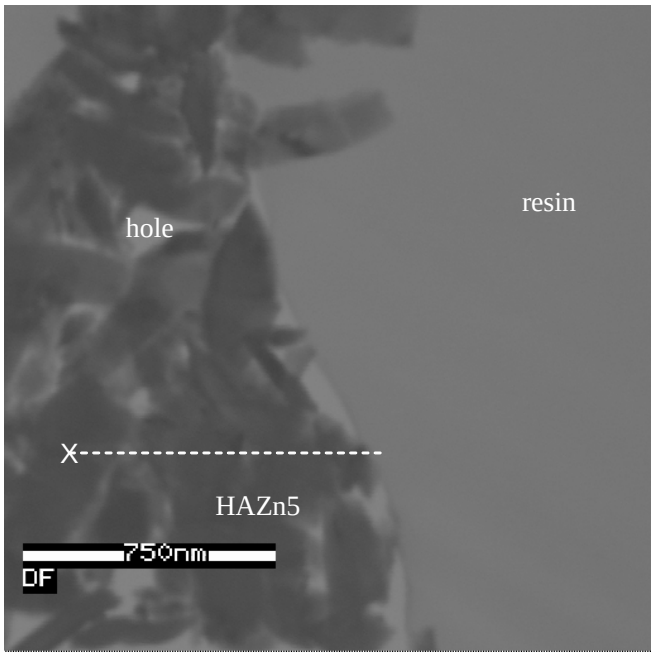

Figure 5

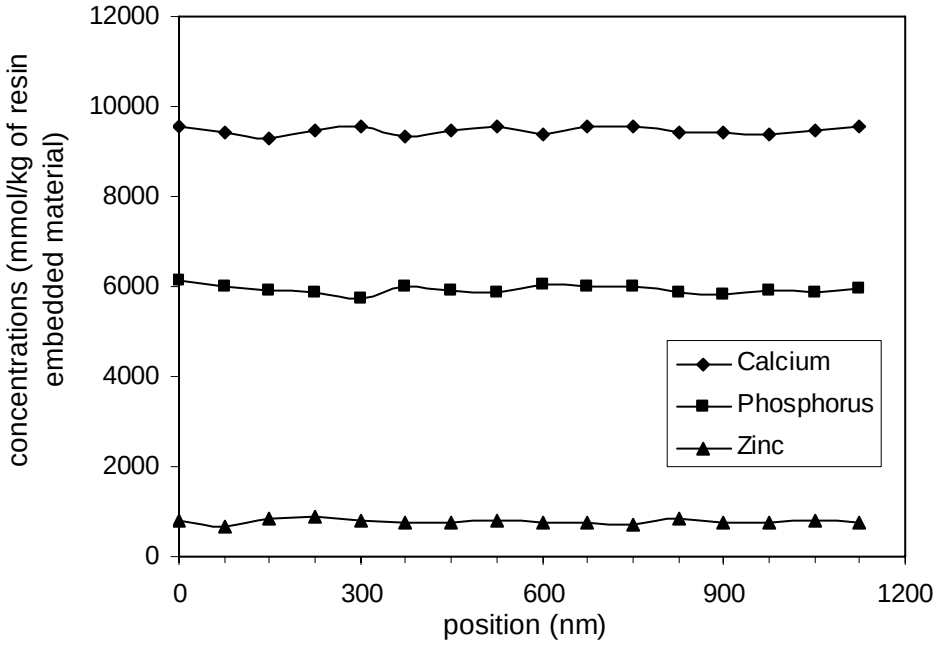

Figure 6

Hal-Inserm Author manuscript

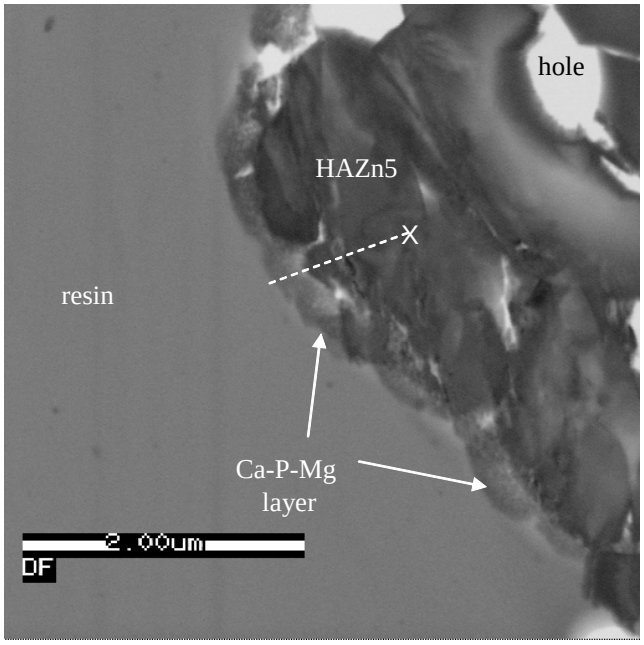

Figure 7

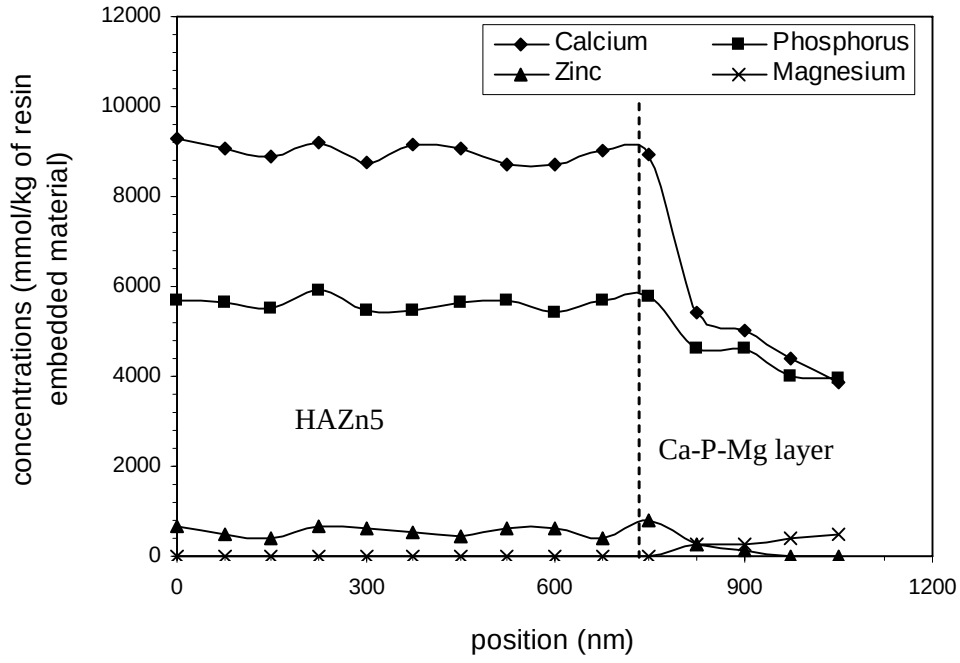

Figure 8